5-2017

Design of an Opposed-piston, Opposed-stroke Diesel Engine for Use in Utility Aircraft

Luke Kozal

Follow this and additional works at: https://ecommons.udayton.edu/uhp_theses

 Part of the Aerospace Engineering Commons, and the Mechanical Engineering Commons

Design of an Opposed-piston, Opposed-stroke Diesel Engine for Use in Utility Aircraft

Honors Thesis

Luke Kozal

Department: Mechanical Engineering

Advisors: Andrew Murray, Ph.D.
David Myszka, Ph.D.
Paul Litke, AFRL/RQTC

May 2017

Design of an Opposed-piston, Opposed-stroke Diesel Engine for Use in Utility Aircraft

Luke Kozal
Department: Mechanical Engineering
Advisor: Andrew Murray, Ph.D.
David Myszka, Ph.D.
Paul Litke, AFRL/RQTC
May 2017

Abstract

The objective of this thesis was to determine the feasibility of using an opposed-piston, opposed-stroke, diesel engine in utility aircraft. Utility aircraft are aircraft that have a maximal takeoff weight of 12,500lbs. These aircraft are often used for transportation of cargo and other goods. In order to handle that weight, many of the aircraft are powered by turboprop engines. Turboprop engines are a style of jet engine with power capabilities ranging from 500 to several thousand horsepower (hp). They are expensive engines, and in the case of the Piper Mirage, substituting the piston engine with a turboprop engine can increase the cost of the aircraft by $1million. In order to reduce the price tag, a piston-powered, propeller engine is desired. Currently, however, most modern piston driven aircraft engines max out around 400hp. The Piper Mirage referenced has a power output of 350hp. Because of this, it was necessary to see if an opposed-piston, opposed-stroke, diesel engine would be able to increase the power output in order to compete with the turboprop engine. The Foundation for Applied Aviation Technology determined that the minimum power output of an opposed-piston, opposed-stroke diesel engine should be 800hp at takeoff at an engine speed of 3600 revolutions per minute (rpm). Opposed-piston, opposed-stroke diesel engines have been used previously in aircraft and perhaps most famously in the Junkers Jumo 205 and 207 engines built in the 1940s. Both of these were opposed-piston, opposed-stroke, diesel engines that generated between 700 and 1000hp at takeoff. However, the Junkers engines were large engines used in large multi-engine aircraft. This thesis determines that the required size for an engine of this output can be reduced by 25% compared to the Junkers engine with a potential weight savings of up to 500lb, a better specific fuel consumption, and a greater power output of over 1200hp.

UNIVERSITY *of*

DAYTON

Table of Contents

1.0 Background

In September 2015, the Foundation for Applied Aviation Technology (FAAT) approached the University of Dayton DIMLab (Design of Innovative Machines Laboratory) with the project of leading the research and development of an opposed piston engine for use in utility aircraft. A utility aircraft is defined by the Federal Aviation Administration (FAA) to be an aircraft that has a maximum takeoff weight of 12,500lbs, must not have more than nine passenger seats and is intended for limited acrobatic operation [1]. This project is motivated by the power gap that exists between turboprop and piston engines. While turboprop engines are the more powerful and lightweight engines, they are extremely expensive. In the case of the Piper Mirage aircraft, the cost of the aircraft with a turboprop engine is a million dollars more than the version of the aircraft with a piston engine [2]. While most piston aircraft typically generate 400hp, it is not uncommon for turboprops to generate 1000hp or more [3]. Because of the significant price difference, the Foundation for Applied Aviation Technology seeks to develop a piston engine that would bridge the power gap between turboprops and piston engines while remaining in the piston engine price bracket. Through the Foundation's research, a market that could benefit significantly from a development in piston engines, is the logging industry in the upper northwest. The Foundation determined that in order for an engine to be of benefit to the industry, it would need to generate at least 800hp. This is a significant increase in power compared to the power normally generated by a piston engine.

In order to accommodate for this significant difference, the opposed piston design was selected in order to meet this power need, see Figure 1. The opposed piston design has been around since 1887, and offers the distinct advantage of being compact, balanced, lightweight, and fuel efficient [4]. Primarily, opposed piston engines also rely on the two-stroke cycle which adds additional benefits to the design which will be the type of engine focused on in this thesis.
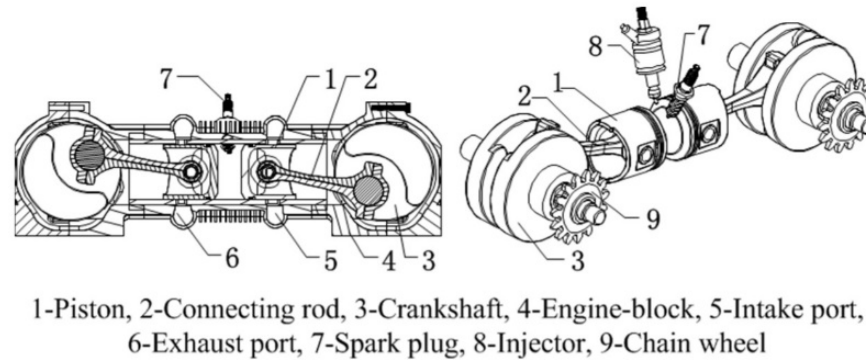
1-Piston, 2-Connecting rod, 3-Crankshaft, 4-Engine-block, 5-Intake port,
6-Exhaust port, 7-Spark plug, 8-Injector, 9-Chain wheel

Figure 1 - Diagram of a Four-stroke, Opposed-piston Engine (Adapted from [11])

1.1 Benefits of the Opposed Piston Two-Stroke Design

The opposed-piston, two-stroke engine has a number of inherent benefits. The first is an increase in power density. This is due to the principal characteristic of the two-stroke engine having a power stroke for every revolution of the crankshaft. Four-stroke engines have a power stroke every two revolutions of the crankshaft. This means that the two-stroke engine is fundamentally more powerful than its four-stroke counterpart [4-6]. Along with being more powerful, because the engine has a combustion event for every rotation of the crankshaft, the cylinder contents are allowed to be leaner than in a four-stroke cycle. This results in lower temperatures throughout the combustion process and therefore a better combustion efficiency. This leads to a 2% increase in fuel efficiency. [7] Additionally, two-stroke engines are diesel engines, which have high compression ratios resulting in greater specific torque [4]. The higher compression ratio also lends itself to greater efficiencies as the compression ratio also allows leaner operating conditions and lower in-cylinder temperatures   Because the cylinder stroke is divided between two pistons, it allows the engine to run at higher speeds without exceeding the limitations of piston speed [5, 8]. This also results in a lowering of the load on the crankshaft due to the forces being shared by two pistons [5]. The two-stroke engine is also inherently lighter than its four-stroke counterpart because the two-stroke cycle uses a loop scavenging system in order to eliminate burned gases from the cylinder after the combustion event. This means that the engine does not need a valve-train with cams. Along with the lack of piston heads, there is a significant reduction in weight. With the reduction in weight, the geometry of the opposed piston engine allows for near perfect

balance [5,6]. Because of this, the two-stroke engine is less complex than the four-stroke due to the nature of the compression ignition process. It does not need piston heads or valve-trains which significantly reduce the number of parts required, the weight of the engine, and the total cost. The total cost reduction is approximately 12%, the total part count is 34% less, and the total weight is 32% less [6]. Lastly, a potential significant benefit especially for the aircraft industry is the ability to use multiple fuels in the engine. A stark example of this was when a Junkers engine flew over 1000 miles on kerosene with no adverse effects [4]. This results in the ability of the engine to use Jet-A fuel instead 100LL aviation gasoline which results in a significant cost benefit especially outside of the United States. A modern example of one of these engines is the Continental CD-135 engine which runs on diesel and Jet-A fuels [9,10].

1.2 Challenges of the Opposed Piston Engine

Although the opposed-piston, two-stroke engine has a number of benefits, it does have its challenges. This first issue is lubrication of the small end-bushes and piston-pin bosses due to the lack of load reversal. There have been solutions to this problem in the past, but none fully alleviated the problem. The solutions typically include special features that distribute the oil to the areas subject to unidirectional loading. Additionally, because of the contiguous firing of the engine, there is a higher thermal load on the engine which in turn can accelerate the wear on the piston rings in an engine. One concept that has been used to alleviate some of this thermal load is "gapless fire-rings" which reduce the friction that is felt on the second and third compression rings. Two-stroke engines have a reputation for needing increased maintenance. In order to avoid this problem, special care needs to be taken in order to ensure that the engines are not undersized for their applications as this will only increase the likelihood of the engine requiring maintenance [4]. The side injection of opposed piston engines also poses the challenge of fuel and air mixing asymmetrically. This also poses the challenge of fuel wetting the cylinder which can also cause lubrication issues and poor combustion. This can be addressed through fuel injection design and ensuring that the proper swirl of fresh charge is obtained [11]. Emissions of the two-stroke engine have also been a serious problem. It is primarily due to the increase in emissions regulations that opposed piston

engines lost their foothold in the market. However, advancements in materials and catalysts have resulted in significant reductions in emissions. It is because of these reductions and the inherent leaner diesel combustion that a renaissance of opposed piston engines has occurred, and a number of recent opposed piston projects have been undertaken [6]. Lastly, and potentially the most serious issue is the problem of oil consumption. This is due to oil being lost through the liner and ports. It is possible to reduce this loss and some marine engines like the Fairbanks Morse engine have oil consumption values close to that of a four-stroke engine [4].

1.3 Examples and Historical Comparison

Because of the noted benefits and proposed solutions to the challenges, the two-stroke engine has been around since the 19th century. Before and during World War II, the Junkers Jumo family of engines was a series of opposed piston diesel engines used in civil and military aviation. It was a vertical opposed piston design. Historically, this was the most broadly used diesel engine in the aviation industry, set a number of records for the industry, and was one of the most efficient piston engine in aviation, see Figure 2 [4]. While opposed piston engines have not been used as much recently, there are projects being undertaken currently. Perhaps, most notably, EcoMotors is planning on releasing an opposed piston, opposed cylinder engine in the near future primarily for use in automobiles.

The Foundation for Applied Aviation Technology set the requirements for the engine to be 800hp at takeoff with a maximum takeoff rpm of 3600. The Jumo Junker family of engines will be used as a model due to similar characteristics and its historical success with dealing with similar requirements. The Junkers Jumo is a family of engines that much of this project will draw information off of due to the power that this family generated. The Junker 207B engine had a takeoff power of 1000 horsepower [4] at 3000rpm while the majority of the other versions had power ratings between 600 and 1000 horsepower at 2600-3000rpm. For the purpose of this thesis, the Junkers 207B will be used as a comparison. It had six cylinders with a weight of 1907lb. It had a brake specific fuel consumption at its most efficient load of 227g/kWh. It had an in-cylinder pressure of 1.88bar and a mean piston speed of 15.11m/s [4]. Because of the success that

the Junkers engine had before and during World War II, it is believed that a two-stroke opposed piston diesel engine can be developed in order to meet or exceed the design requirements laid out by the Foundation.
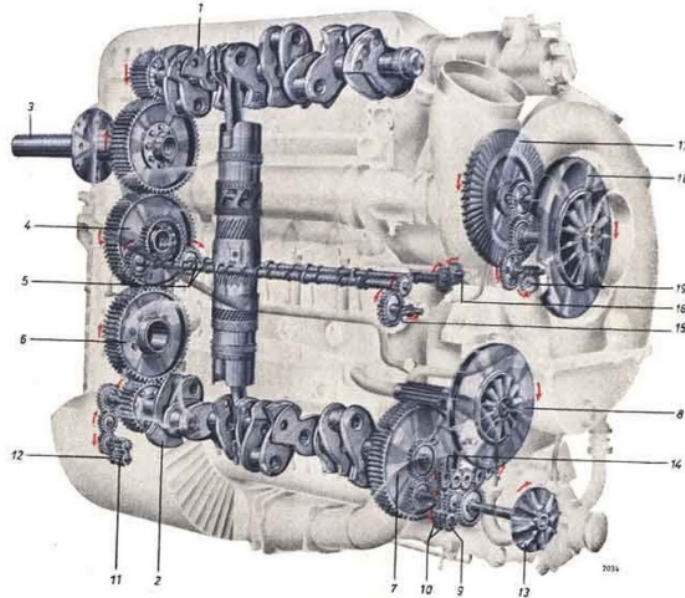
Figure 2 - Ghost View of a Junkers 205 Engine (adapted from [OPE])

2.0 Simulation Model Used to Determine Feasibility of Engine

In order to determine if the two-stroke diesel engine would be a possibility the engine needed to first be sized. This means that the geometrical aspects of the engine needed to be determined. These aspects include: the number of cylinders, the volume contained within each cylinder, and the stroke and bore lengths for each cylinder. In order, to determine these characteristics the equation for mean effective pressure was utilized: [12]

$$mep = \frac{Pn_r}{V_d N} \tag{1}$$

Where P is the power, n_r is the number of crankshaft revolutions per combustion event, V_d is the displaced volume, and N is the speed of the engine. Mean effective pressure is a value that shows how well the displaced volume within the cylinder is being utilized. This means that mean effective pressure does not depend on the size of the engine and it can be used to compare engines of different volumes [12]. Additionally, this means that

compression ignition engines will have specific ranges of *mep* in which they will fall. Because the plan is to have a turbocharger for the final design, a mean effective pressure value was chosen from standard turbocharged compression ignition mean effective pressure values.

   Knowing this volume, it can be determined how large the bore and stroke should be within the engine. As a general rule, mean piston speeds should not exceed 15 m/s [12]. This is due to friction losses and in order to reduce wear that will be incurred over the course of the engines life.   The equation for mean piston speed is:

$$\bar{S}_p = 2LN \tag{2}$$

Where *L* is the stroke length. The reason why stroke length was focused on and not bore is due to the nature of combustion efficiency. The greater the ratio of stroke to bore, the better combustion efficiency will become. This results in a fuel conversion efficiency and therefore a better overall fuel economy. This means that the aircraft will have a lesser need for fuel which is extremely beneficial in aviation as it either leads to weight savings or a greater range of travel.

   With the geometrical values for the engine calculated, it needed to be determined if the engine would perform the way the mean effective pressure equation predicted. In order to determine this, the 0D model that was used in the by paper by R. E. Herold et al's assessment of the thermal benefits of opposed-piston, two-stroke diesel engines was recreated [7]. This model was chosen due to its simplicity of design in order to validate the previous equations. The purpose of the model is to determine the pressure value at every crank angle degree (CAD) within an engine cycle. This model also assumes a prewarmed engine and ideal gases within the cylinder. Unlike an ideal cycle, this model takes into account three different aspects of heat and energy release during combustion. These aspects include the combustion energy release, $\frac{dQ_c}{d\theta}$, and the heat release due to the surfaces within the cylinder, $\frac{dQ_{HT}}{d\theta}$. Additionally, the cycle, takes into consideration the change in fluid composition within the cylinder. This is done by recompleting the equilibrium balance for each crank angle. However, this model does not include friction. Because the literature compared three different engine geometries with identical dimensions, friction was ignored as it should be the same for each geometry [7].

The basis for the 0D model is a closed system energy balance where combustion is assumed to be ideal gas based with an energy addition. The resulting equation is:

$$\frac{dp}{d\theta}\bigg|_i = \left(\frac{dQ_c}{d\theta}\bigg|_i - \frac{dQ_{HT}}{d\theta}\bigg|_i - \frac{\gamma_i}{\gamma_i-1}p_i\frac{dV}{d\theta}\bigg|_i\right)\frac{\gamma_i-1}{V_i} \tag{3}$$

Where $\frac{dp}{d\theta}\big|_i$ is the change in pressure within the cylinder relative to the crank angle i.

Gamma is the ratio of specific heats of the gases within the cylinder. $\frac{dV}{d\theta}\big|_i$ is the change in volume per crank angle and V_i is the volume at a specific crank angle degree [7].

$\frac{dQ_c}{d\theta}\big|_i$ is the energy addition due to combustion and it is defined by the equation:

$$\frac{dQ_c}{d\theta}\bigg|_i = \frac{x_{b,i+1}-x_{b,i-1}}{\theta_{i+1}-\theta_{i-1}}\left(m_f LHV_f\right) \tag{4}$$

Where $x_{b,i}$ is the mass burn fraction rate, m_f is the mass of the injected fuel and LHV is the lower heating value of the fuel [7]. The mass of the fuel injected is dependent on the air fuel ratio, and the lower heating values for fuels are tabulated in most textbooks. The lower heating value for diesel fuel is 42.5 MJ [12]. The mass burn fraction rate is an equation that matches how much fuel is burned per crank angle degree between the start of injection and the end of combustion. It is defined by the equation:

$$x_{b,i} = 1 - \exp\left\{-\left[\left(2.302^{\frac{1}{m_c+1}} - 0.105^{\frac{1}{m_c+1}}\right)\left(\frac{\theta_i-\theta_{SOC}}{\Delta\theta_{10-90}}\right)\right]^{m_c+1}\right\} \tag{5}$$

Where m_c is the Wiebe combustion exponent and is given a value of 0.7 [7]. $\Delta\theta_{10-90}$ is the value for the number of crank angle degrees that it will take for the fuel to burn. θ_{SOC} is the crank angle degree at which combustion begins [7,12].

$\frac{dQ_{HT}}{d\theta}\big|_i$ is the heat transfer due to the surfaces inside of the cylinder. It is defined by the equation:

$$\frac{dQ_{HT}}{d\theta}\bigg|_i = h_{c,i}\left[A_{IP,i}\left(T_i - T_{m,IP}\right) + A_{EP,i}\left(T_i - T_{m,EP}\right) + A_{l,i}\left(T_i - T_{m,l}\right)\right] \tag{6}$$

Where h_{ci} is the convective heat transfer coefficient. $A_{IP,i}$, $A_{EP,i}$ and $A_{l,i}$ are the surface areas of the surfaces inside the cylinder, and $T_{m,IP}$, $T_{m,EP}$, and $T_{m,l}$ are the mean temperatures of the surfaces of the cylinder. The surfaces inside the cylinder referenced are the intake piston, the exhaust piston, and the liner. T_i is the temperature of the gases inside the cylinder that is calculated using the assumption of ideal gases. h_{ci} is a term

that depends on the speed of the gases within the cylinder and other factors and is defined by the following equation:

$$h_{c,i} = 5B^{m_{ht}-1} p_i^{m_{ht}} w_i^{m_{ht}} T_i^{0.75-1.62m_{ht}} \tag{7}$$

Where B is the bore of the cylinder. p_i is the pressure at the current crank angle. The m_{ht} exponent found in this equation is the Woschni exponent and is given a value of .8 [7,12]. The convective heat transfer coefficient is important because it is responsible for determining how fast energy is transferred from the gases into the surrounding surfaces. w_i is speed of the gases within the cylinder and is defined by the Woschni correlation:

$$w_i = C_1 \bar{S}_p + C_2 \frac{V_d T_o}{p_o V_r}(p_i - p_{mot,i}) \tag{8}$$

Where C_1 and C_2 are constants and are equal to 2.28 and 0 for the compression phase of the cycle and 2.28 and 3.24x10^{-3} for the expansion phase respectively [12]. V_d is the displaced volume within the cylinder. V_r, To and Po are a reference volume, temperature and pressure at some arbitrary point within the cycle like when the ports close. p_{mot} is the motoring pressure. $\bar{S}_p$ is the mean piston speed as defined in Equation 2. The motoring pressure is calculated the same as the compression part of the cylinder except with zero energy release [7].

In order to determine the last part of the $\frac{dp}{d\theta}\big|_i$ equation which accounts for the internal energy change, the gamma term needs to first be determined. Gamma is determined by the equation:

$$\gamma_i = \frac{c_{p,i}}{c_{p,i} - R_i} \tag{9}$$

Where $c_{p,i}$ is the specific heat of the gas mixture within the cylinder at the specific CAD and R_i is the specific gas constant for the gases within the cylinder at the CAD. c_p is defined by the equation:

$$c_{p,i} = \sum_{j=1}^{n} y_{j,i} c_{p,j,i} \tag{10}$$

Where $y_{j,i}$ is the mass fraction of a gas element within the cylinder and $c_{p,j,i}$ is the specific heat of that element. $c_{p,j,i}$ is defined by the specific heat capacity curve:

$$c_{p,n,i} = R_n \sum_{j=1}^{7} a_{j,n} T_i^{j-3} \tag{11}$$

Where R_n is the specific gas constant for the 4 constituents of the gases within the cylinder. $a_{j,n}$ is the specific heat coefficient as published by NASA Glenn to fit this curve

[7]. The constituents are O_2, N_2, CO_2, and H_2O. The chart of coefficients was provided in the literature. This assumes complete combustion and that the composition is frozen within the cylinder [7]. Temperature at each CAD is defined using the ideal gas equation:

$$T_i = \frac{p_i V_i}{m_i R_i} \tag{12}$$

Where m_i is the mass of the gases within the cylinder at the CAD. At the start of fuel injection, the mass will increase by the amount of fuel injected. The specific gas constant for the cylinder gases, R_i, is defined as:

$$R_i = \frac{\bar{R}}{MW_i} \tag{13}$$

Where $\bar{R}$ is the ideal gas consant and MW is the specific molecular weight of the gas mixture inside of the cylinder. MW takes into consideration the mole fractions of the various constituents within the cylinder at various crank angles and is defined as:

$$MW_i = \sum_{j=1}^{n} x_{j,i} MW_{j,i} \tag{14}$$

Where $MW_{j,i}$ is the molecular weight of the individual gases and $x_{j,i}$ is the mole fraction of that particular gas. By summing these fractions, one is able to come to the total molecular weight of the cylinder gases. The mole fraction of each element is defined by the equation:

$$x_{n,i} = x_{n,o}(1 - x_{b,i}) + x_{n,b}(x_{b,i}) \tag{15}$$

Where $x_{n,o}$ is the mole fraction of the specific element before complete combustion. $x_{b,o}$ is the mole fraction of the element after complete combustion. From this equation, the mass fraction for each element can be determined by the equation:

$$y_{n,i} = x_{n,i} \frac{MW_{n,i}}{MW_i} \tag{16}$$

Where $MW_{n,i}$ is the molecular weight for the specific element [7].

In order to determine the volume at a particular CAD, the following equation from Heywood was used:

$$\frac{V(\theta)}{V_c} = 1 + \frac{1}{2}(r_c - 1)[R + 1 - cos\theta - (R^2 - sin\theta^2)^{0.5}] \tag{17}$$

Where V_c is the clearance volume and R is the ratio of connecting rod to crankshaft throw, and r_c is the compression ratio [12]. The compression ratio is defined as:

$$r_c = \frac{V_d + V_c}{V_c} \tag{18}$$

Where V_d is the volume that the piston displaces during a cycle. The derivative of the volume is defined to be:

$$\frac{dV}{d\theta}\bigg|_i = \frac{V_{i+1}-V_{i-1}}{\theta_{i+1}-\theta_{i-1}} \tag{19}$$

With this equation, all of the components for the change in pressure have been defined [7]. In order to determine the pressure at the next CAD, the change in pressure is added to the previous pressure value as defined in the following equation:

$$p_{i+1} = p_i + \frac{dp}{d\theta}(\theta_{i+1} - \theta_i) \tag{20}$$

Using the aforementioned equations, one can determined how the pressure changes during a combustion cycle assuming that the gases are ideal and that combustion occurs completely with the constituents being frozen [7].

In order to calculate the dimensions of the ports that allow air into and out of the cylinder the volumetric flow rate equation:

$$Q = vA \tag{21}$$

was used where Q is the volumetric flow rate, v is the velocity of the air, and A is the area of the port. The v was determined using Equation 8 for the velocity of in-cylinder gases during the compression phase.

After calculating the port sizes, the turbocharger needed to be sized. Because turbochargers are sized by the mass flow rate of air that flows through them, the mass flow rate of air was determined using the air fuel ratio equation:

$$AFR = \frac{\dot{m}_a}{\dot{m}_f} \tag{22}$$

Where AFR is the air fuel ratio, $\dot{m}_a$ is the mass flow rate of air, and $\dot{m}_f$ is the mass flow rate of fuel [12,13]. The air fuel ratio can be determined from the 0D model as it is directly related to the lambda value. Lambda is the mass based ratio of the stoichiometric air fuel ratio to the actual air fuel ratio. A lambda value of 1 practically means that there is roughly one molecule of fuel for every molecule of air. The standard value for the stoichiometric air fuel ratio of diesel is 14.45 [12]. Diesel engines are run lean meaning that there is more air than fuel in the cylinder and a typical lambda value is 1.43. Lambda is defined with the following equation:

$$\lambda = \frac{AFR_a}{AFR_s} \tag{23}$$

Where AFR_a is the actual air fuel ratio and AFR_s is the stoichiometric air fuel ratio.

In. order to determine the total power output of the engine, the following equation was used:

$$P = N_c \frac{\sum_i^n p_i \frac{dV}{d\theta}\big|_i}{t_s} \tag{24}$$

Where P is the power, p_i is the pressure at a specific CAD and $\frac{dV}{d\theta}\big|_i$ is the change in volume at that same step. t_s is the length of time for a single cycle to occur, and N_c is the number of cylinders within the engine.

Lastly, the specific fuel consumption could be calculated. This is an important value to compare between aircraft engines and is determined using the following:

$$sfc = \frac{\dot{m}_f}{P} \tag{25}$$

where $\dot{m}_f$ is the fuel flow rate and P is the power output of the engine. The mass flow rate of fuel can also be determined from the 0D model as the mass of the fuel is related to the lambda value as well. This value shows how well the engine is taking the fuel and converting it to usable power [12].

3.0 Results and Discussion

The volume for the desired engine was determined using the equation for mean effective pressure, Equation 1. The mean effective pressure that was chosen was 140psi as it coincided with mean effective pressures for turbocharged two-stroke diesel engines at maximum power [12]. The Foundation for Applied Aviation Technology specified the other inputs of 800hp and a 3600rpm takeoff engine speed. This results in a displaced volume of 10.3004 liters. Using the takeoff engine speed and the maximum mean piston speed, the maximum stroke length could be determined using the mean piston speed Equation 2. This resulted in a stroke length of 125mm. Using the stroke length, the bore length could be determined and its size depends on the number of cylinders desired. In order to keep the bore diameter reasonably small, six cylinders were decided upon. This results in a bore of 92.5mm.

In order for a two-stroke diesel engine to be successful, it needs a crankshaft offset to have effective scavenging. A crankshaft offset is the difference in CAD that the pistons are operating at within the cylinder. This offset allows the intake and exhaust ports to open at different crank angles allowing for the exhaust gases to escape before the fresh air is inducted. Like the model that was used in the literature model and in many other opposed piston engines, an offset of 13.5 degrees was chosen [7]. Because of this offset, it meant that the length of the cylinder was shortened because one piston would always be 13.5 degrees ahead of the other. In order to compensate for the loss of volume, the bore was expanded from 92.5mm to 96.1mm. Additionally, once the port dimensions were determined, it resulted in an even further reduction of trapped volume within the cylinder. Since the maximum cylinder length was limited by the maximum stroke length of 125mm, the available surface area on the cylinder was compared to the area needed for the ports and then the bore was readjusted in order to meet the needed port area. This resulted in the bore increasing from 96.1mm to 100mm. After the adjustments to the bore, the trapped volume remained 10.3L in order to match the displaced volume calculated using Equation 1. The total volume, however, increased to 12.3L since the total volume includes the volume occupied by the ports. 12.3L is still 25% smaller than the Junkers Jumo 207B. This also changed the stroke to bore ratio from 1.35 to 1.25.

In order to determine the size of the ports, the volumetric flow rate equation, Equation 21, was used. The velocity of the cylinder gases was calculated using Equation 8 from for the compression portion of the cycle. The volumetric flow rate was determined by using the 10.3L of trapped volume and dividing it by the cycle time. This resulted in an intake port area of 30cm^2 per cylinder. Because the exhaust port area is roughly 30% larger than the intake, the exhaust port area was then 39cm^2. This value was still smaller than the Junkers values and left a lot of closed space around the cylinder. Because of this, the total port area was increased to be more proportional to that of the Junkers engine. This resulted in intake and exhaust port areas of 39cm^2 and 45cm^2. [4]. The extra area will only positively affect scavenging; as the greater the port area, the better the air flow.

Once the general dimensions of the engine were determined, a model could be chosen to determine more accurately what the actual output of the engine would be. In

order to do this, the 0D model from the literature was constructed [7]. This model was used to demonstrate the thermodynamic benefits of the opposed-piston, two-stroke engine. However, one downside from this model was that the model does not include friction. The result of this is that the indicated values calculated will be slightly inflated compared to what they would be if friction was accounted for. Therefore, the literature's 0D model was used to validate whether or not the mean effective pressure equation accurately determined the size of the engine and the potential power output of the engine itself. Because the original model that was used in the paper was unavailable, it needed to be constructed for this thesis and validated. The engine that was run in the literature was an opposed-piston, two-stroke diesel that obtained 300hp at 2400rpm. A chart of the output values along with its running conditions can be seen in Figure 3.

Condition	Peak Power
Engine Speed (rpm)	2400
Indicated Power (hp)	300
Trapped Pressure (bar)	2
Trapped Temp. (K)	350
Trapped Composition	Air
Piston/Head Metal Temp. (K)	550
Liner Metal Temp. (K)	450
CA10 (deg aTDC)	0
MPRR (bar/deg)	5.1

Figure 3 - Geometry of Simulation Model [7]

Additionally, the geometry of the simulation model was copied and its values can be seen in Figure 4.

Engine	OP2S
Cylinder Count	3
Bore (mm)	102.6
Stroke per Piston (mm)	112.9
Engine Stroke (mm)	224.2
Trapped Volume (L/cylinder)	1.6
Total Trapped Volume (L)	4.8
Trapped Compression Ratio	15:1
Clearance Volume (mm3)	1.1e5
Crank Radius (mm)	56.4
Connecting Rod Length (mm)	197.5
Pin-to-Crown Distance (mm)	60
Head-to-Crank Distance (mm)	---
Crank-to-Crank Distance (mm)	639.8
Crankshaft Phase Offset (deg)	13.5
Intake Closing (deg aTDC)	-120
Exhaust Opening (deg aTDC)	120

Figure 4 - Dimensions of the simulation engine (adapted from [7])

Because the original model was unavailable and it needed to be reconstructed for use in this thesis, care was taken in order to take into account each of the values from the values in the literature. For the sake of simplicity, the model was built for a single cylinder meaning that the target power output was 100hp instead of 300hp. A minor difference that originated from the reconstruction was that the port openings occurred at ±126 CAD and not at ±120 like in the paper. In the reconstructed model, it was found where the trapped volume was 1.6L, but this occurred at -126 degrees. After carefully looking through the volume equations, it could not be determined why there was a difference in the port openings compared to the paper. In order to build the model, Microsoft Excel was used. Several tabs were utilized in order to properly account for equations noted in section 2 of this paper. One tab was used for the calculations of the governing equation and heat transfer, Equations 3 and 6, another was used for volume calculations, Equation 17, a third was used for combustion, Equation 4, a fourth was used to determine gamma, Equation 9, and a fifth was used for determining the specific heat for each element in Equation 11. Figure 5 shows a screenshot of the overall program.

Parameters:

Bore	0.1026	[m]
Stroke	0.1129	[m]
R	3.5	
mht	0.8	
C1	2.28	
C2	0	
C3	3.25E-03	
Vd	0.002	[m^3]
Tr	350	[K]
Vr	0.001525592	[m^3]
Pr	200000	
N	2400	[rpm]
Sp	9.032	[m/s]
Aip	0.008267698	[m^2]
Aep	0.008267698	[m^2]
Tip	550	[K]
Tep	550	[K]
Tl	450	[K]
Rho_Air	1.991040319	kg/m^3
ma_cylinder	0.003171555	[kg]
Theta_Time	6.94444E-05	[s]
Cell Start	56	

Summary of Collected Data

	My Data	Fosters
Lambda = 2.68		
Total Work - 1cyl	1911.9	
Total Power [kW]	76.4762	
Total Power [Hp]	102.556	100
6Cyl. Power	307.669	300
MPRR	2.68441	5.1
Max Pressure Bar	83.315	121
Max m-Pressure	68.3215	80
Max Temperature	1619.29	1724

Crank Angles	A-liner [m^2]	Temperature [K]	Pressure [Pa]	[Bar]	dPdTheta [Pa]	dQHTdTheta [J]	hci [W/(m^2 K)]	wi [m/s]	dQCdTheta [J]	DpDTheta_Motor	Pressure Bar	Work
-126	0.062434288	348.4498153	200000	2	2154.429777	-0.165028052	245.6758222	20.59296	0	2113.37714	200000	2	0
-125	0.061958476	349.5192223	202154.4298	2.02	2225.226449	-0.163896329	247.3734448	20.59296	0	2183.77701	202113.3771	2	-2.49
-124	0.06147575	350.6134512	204379.6562	2.04	2298.483937	-0.162738122	249.1207879	20.59296	0	2256.62303	204297.1541	2	-2.55
-123	0.060986185	351.7329765	206678.1402	2.07	2374.31497	-0.161552875	250.9192558	20.59296	0	2332.02792	206553.7772	2.1	-2.61
-122	0.060489861	352.878286	209052.4551	2.09	2452.838039	-0.16034001	252.7703072	20.59296	0	2410.11021	208885.8051	2.1	-2.68
-121	0.059986861	354.049881	211505.2932	2.12	2534.177744	-0.159098929	254.6754583	20.59296	0	2490.99456	211295.9153	2.1	-2.75
-120	0.059477271	355.2482766	214039.4709	2.14	2618.465157	-0.157829012	256.6362845	20.59296	0	2574.81217	213786.9099	2.1	-2.82
-119	0.058961182	356.4740022	216657.9361	2.17	2705.838219	-0.156529617	258.6544235	20.59296	0	2661.70116	216361.722	2.2	-2.89
-118	0.058438689	357.727602	219363.7743	2.19	2796.442152	-0.155200077	260.7315777	20.59296	0	2751.80698	219023.4232	2.2	-2.96
-117	0.05790989	359.0096348	222160.2164	2.22	2890.429911	-0.153839699	262.8695173	20.59296	0	2845.2829	221775.2302	2.2	-3.03
-116	0.057374887	360.3206751	225050.6464	2.25	2987.962655	-0.152447766	265.0700831	20.59296	0	2942.29046	224620.5131	2.2	-3.11
-115	0.056833787	361.6613129	228038.609	2.28	3089.210259	-0.151023532	267.3351898	20.59296	0	3043	227562.8035	2.3	-3.18
-114	0.056286701	363.0321546	231127.8193	2.31	3194.351856	-0.149566221	269.6668294	20.59296	0	3147.59123	230605.8035	2.3	-3.26
-113	0.055733744	364.4338232	234322.1711	2.34	3303.576417	-0.148075029	272.0670744	20.59296	0	3256.25381	233753.3948	2.3	-3.34
-112	0.055175035	365.8669586	237625.7475	2.38	3417.083373	-0.146549119	274.538082	20.59296	0	3369.18796	237009.6486	2.4	-3.42
-111	0.054610698	367.3322184	241042.8309	2.41	3535.083278	-0.14498762	277.0820974	20.59296	0	3486.6052	240378.8365	2.4	-3.51
-110	0.05404086	368.8302781	244577.9142	2.45	3657.798522	-0.143389626	279.7014586	20.59296	0	3608.72903	243865.4417	2.4	-3.59
-109	0.053465654	370.3618317	248235.7127	2.48	3785.464087	-0.141754194	282.3986002	20.59296	0	3735.7957	247474.1708	2.5	-3.68
-108	0.052885217	371.9275924	252021.1768	2.52	3918.328363	-0.14008034	285.1760581	20.59296	0	3868.0551	251209.9665	2.5	-3.77
-107	0.052299688	373.5282928	255939.5052	2.56	4056.654023	-0.138367042	288.0364748	20.59296	0	4005.77161	255078.0216	2.6	-3.86
-106	0.051709215	375.1646854	259996.1592	2.6	4200.718954	-0.136613231	290.9826038	20.59296	0	4149.22505	259083.7932	2.6	-3.95
-105	0.051113946	376.8375438	264196.8781	2.64	4350.817257	-0.134817793	294.0173153	20.59296	0	4298.71176	263233.0182	2.6	-4.05
-104	0.050514035	378.5476624	268547.6954	2.69	4507.260327	-0.132979566	297.1436022	20.59296	0	4454.54568	267531.73	2.7	-4.15
-103	0.049909642	380.2958578	273054.9557	2.73	4670.377997	-0.131097335	300.3645857	20.59296	0	4617.05952	271986.2757	2.7	-4.25
-102	0.049300929	382.0829687	277725.3337	2.78	4840.519779	-0.129169832	303.6835216	20.59296	0	4786.60607	276603.3352	2.8	-4.35
-101	0.048688064	383.9098572	282565.8535	2.83	5018.056188	-0.12719573	307.1038076	20.59296	0	4963.55955	281389.9413	2.8	-4.46
-100	0.048071219	385.7774091	287583.9097	2.88	5203.380168	-0.125173641	310.6289897	20.59296	0	5148.31707	286353.5008	2.9	-4.56
-99	0.047450569	387.6865344	292787.2899	2.93	5396.908615	-0.123102113	314.2627702	20.59296	0	5341.30026	291501.8179	2.9	-4.67
-98	0.046826294	389.6381685	298184.1985	2.98	5599.084026	-0.120979624	318.0090152	20.59296	0	5542.95693	296843.1181	3	-4.79
-97	0.046198581	391.6332725	303783.2825	3.04	5810.376262	-0.118804578	321.8717635	20.59296	0	5753.76292	302386.0751	3	-4.9
-96	0.045567617	393.672834	309593.6588	3.1	6031.284439	-0.116575305	325.8552351	20.59296	0	5974.22408	308139.838	3.1	-5.02
-95	0.044933595	395.7578682	315624.9432	3.16	6262.338976	-0.11429005	329.9638406	20.59296	0	6204.87838	314114.0621	3.1	-5.14
-94	0.044296712	397.889418	321887.2822	3.22	6504.103781	-0.111946969	334.2021914	20.59296	0	6446.29822	320318.9404	3.2	-5.27
-93	0.04365717	400.0685556	328391.386	3.28	6757.178611	-0.109544128	338.5751099	20.59296	0	6699.09287	326765.2387	3.3	-5.4

Figure 5 - 0D Model Excel Overview

In the figure one can see how all of the values throughout the program relate to a single crank angle. The reason why excel was used was due to the programs inherent structure as each cell could be related to a specific CAD and determine the respective pressure change. The results can be seen in Figure 8.

To verify that the model was accurate, several items were looked at. The first was the volume per crank angle which can be seen in Figure 6.
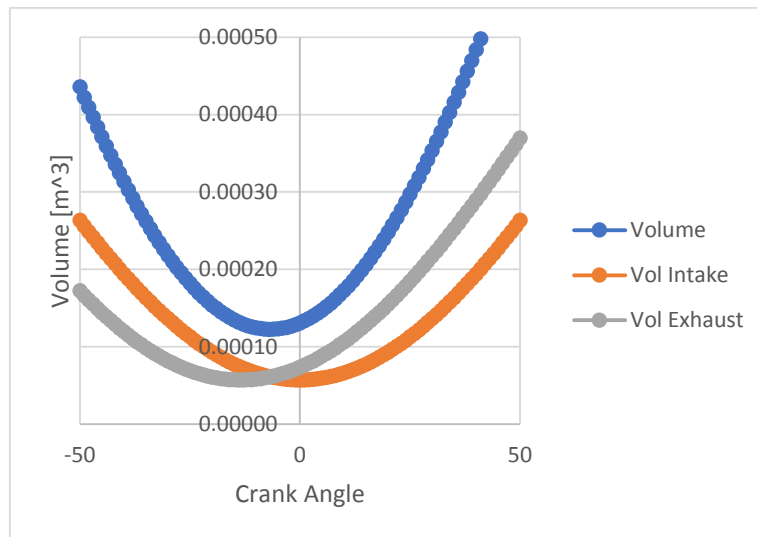

Figure 6 - Volume per Crank Angle

As expected, because the exhaust volume is offset 13.5 degrees, it reaches its minimum volume at -13.5 degrees relative to top dead center and the intake volume reaches its minimum at top dead center. Because of this, the clearance volume is present not at top dead center like an engine without an offset but at -6.75 degrees.

Along with the volume of the system, Equation 5 was also an important aspect of the program that needed to be verified. This equation was an integral aspect of the program as it relates the rate at which energy is released during the combustion cycle. Not only is it included in the combustion equation, Equation 4, but also in Equation 15 which determines the mole fraction of each element in the cylinder. In the paper, it stated that the start of combustion was adjusted so that at 0 CAD, 10% of the energy had been released which means that the value of $x_{b,i}$ should be 0.1 at 0 CAD [7]. In Figure 7, one can see the graph of Equation 5 and how at 0 degrees it has value of 0.1 at 0 CAD.
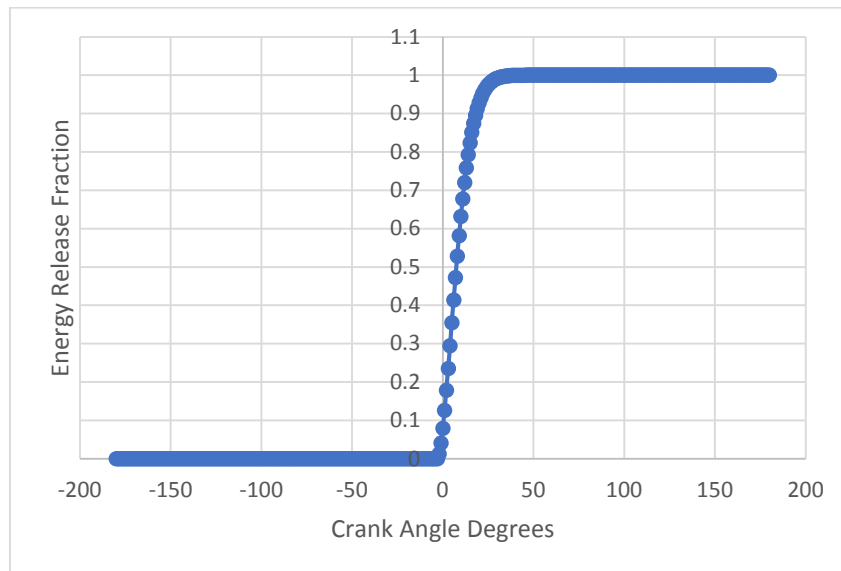

Figure 7 – Graph of Equation 5

The third value that needed to be verified against the simulation model before the results could be calculated was the value of gamma throughout the cycle. Figure 8 shows the values determined from the reconstructed 0D model with those of the literature [7]. It demonstrates that the values calculated for this thesis matched the values from the literature. The yellow line is the line of values determined using the model built for this thesis. The green line is the line of the opposed-piston, two-stroke engine analyzed in the literature.
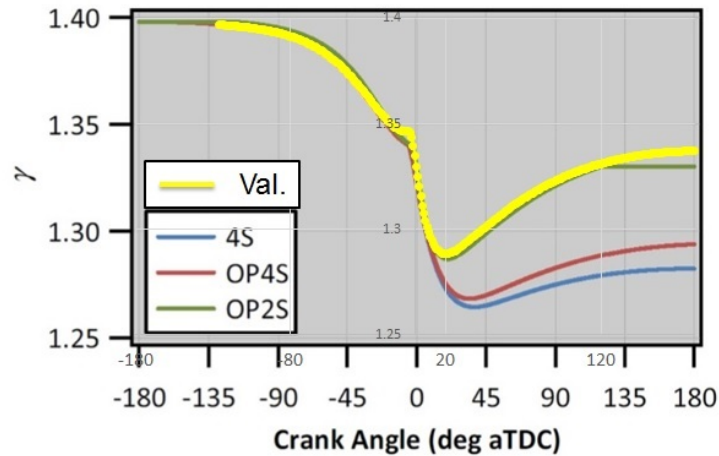
Figure 8 *- Gamma vs Crank Angle (adapted from [7])*

Once these graphs were validated, the program could be run to determine whether or not the model functioned as expected. In order to do so, a graph of the pressure values compared to the crank angle was generated and overlaid on a graph from the literature itself [7]. The result was that the 0D model constructed for this thesis was accurate in all areas except during the combustion portion of the cycle. The resulting graph can be seen in Figure 9. The yellow line is results from the 0D model for this thesis. The green line is the results of the opposed-piston, two-stroke from the literature [7].
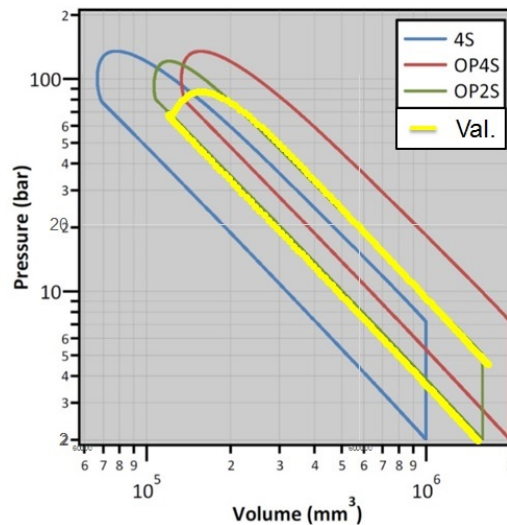

Figure 9 *- Pressure vs Volume Diagram (adapted from [7])*

From this figure, one can see that the values calculated for this thesis were very close, but lost some accuracy near the combustion portion of the cycle. The comparison of the results in Figure 10, show that the power outputs were nearly identical with power

output being 102.6hp per cylinder compared to the literature's 100hp per cylinder. Additionally, the maximum temperature was 1619K compared to the 1724K in the literature. However, the maximum pressure was only 83bar compared to the literature's 121bar [7]. Both models were run at a lambda value of 2.68 and the had $\Delta\theta_{10-90}$ values of 17.8 degrees [7]. Extensive time was spent in order to find solutions to the discrepancies between the values in the literature and the values from the model used for this literature; however, no solution was able to be found.

Engine	OP2S
Fuel Mass (mg/cycle/cyl)	81.8
$\Delta\theta_{10\text{-}90}$ (deg)	17.8
Peak Pressure (bar)	121
Peak Temp. (K)	1724
Trapped λ	2.68

Reconstructed 0D Model	
Fuel Mass	82.3
$\Delta\theta_{10-90}$ **(deg)**	17.8
Peak Pressure Bar	83.17
Peak Temp. [K]	1619
Trapped lambda	2.68
Power [hp]	307.67
MPRR	2.68

Figure 10 - Results of the Literature [7] Engine Simulation vs Literature Values

Because the total power output was nearly identical with the literature along with the gamma values, volume, and Equation 5, it was deemed that the reconstructed 0D model could be used to generate data for the desired engine. Once this decision was made, the dimensions that were determined using the mean effective pressure equations and mean piston speed equations were input into the 0D model. For the combustion portion of the model, 17.8 degrees remained as the value for $\Delta\theta_{10-90}$ in Equation 5 as that was the value that was used in the literature in order to obtain a max pressure rise rate of 5.1bar/degree [7]. For spark ignition engines, a pressure increase of 5.1bar/degree is about the maximum allowable. The literature chose this value in order to compare the 2S diesel design with SI engines [7]. Diesel engines are able to withstand maximum pressure rise rates of about 10bar/degree so having a fast burn rate is not detrimental to the engine. Additionally, the start of combustion was adjusted to have released 10% of the energy at zero CAD like in the literature [7]. The value for m_c in Equation 5 was kept at .7 as that was consistent with the paper and textbooks [12]. Lastly, the lambda value was changed from 2.68 in the literature to 1.9. This was done in order to better reflect a standard diesel's lambda value of 1.43. 1.9 is still a very lean air fuel mixture, but not as

lean as the value used in the literature [7]. The resulting tab and $x_{b,i}$ graph can be seen in Figures 11 and 12.

|	A	B	C	D Crank Angle	E Xbi	F Xbi_corrected	G mc+1	H cst^mc	I Thetas	J	K Mass Air	L Change Ma	M dQCdTheta
1				Crank Angle	Xbi	Xbi_corrected	mc+1	cst^mc	Thetas		Mass Air	Change Ma	dQCdTheta
176	Constants			-6	#NUM!	0.0000	#NUM!	1.3675	-0.1264		0.00298964	0	0
177	mc	0.7		-5	#NUM!	0.0000	#NUM!	1.3675	-0.0702		0.00298964	0	0
178	Theta SOC	-3.75		-4	#NUM!	0.0000	#NUM!	1.3675	-0.0140		0.00298964	0	18.01387
179	Theta10-90	17.8		-3	0.00778	0.0078	0.0078	1.3675	0.0421		0.00298964	1.81487E-05	75.11342
180	CAD - 0 xbi	0.1136		-2	0.03246	0.0325	0.0330	1.3675	0.0983		0.003007789	1.81487E-05	140.9158
181	CAD - 0 dQdT	222.608938		-1	0.06868	0.0687	0.0712	1.3675	0.1545		0.003025937	1.81487E-05	187.6932
182	Vd	0.00171605		0	0.11357	0.1136	0.1206	1.3675	0.2107		0.003044086	1.81487E-05	222.6089
183	Po	175000	[m^3]	1	0.16489	0.1649	0.1802	1.3675	0.2669		0.003062235	1.81487E-05	247.8358
184	Rho_air	1.74216028	[Pa]	2	0.22068	0.2207	0.2493	1.3675	0.3230		0.003080383	1.81487E-05	264.6315
185	mass air	0.00298964	[kg/m^3]	3	0.27925	0.2792	0.3275	1.3675	0.3792		0.003098532	0	274.015
186	mass air_2.0	0.00348432	[kg]	4	0.33910	0.3391	0.4141	1.3675	0.4354		0.003098532	0	276.9407
187	FAR_S	0.06920415		5	0.39893	0.3989	0.5090	1.3675	0.4916		0.003098532	0	274.3452
188	Lamba	1.9		6	0.45766	0.4577	0.6119	1.3675	0.5478		0.003098532	0	267.149
189	Phi	0.52631579		7	0.51438	0.5144	0.7223	1.3675	0.6039		0.003098532	0	256.2448
190	FAR_A	0.03642324		8	0.56840	0.5684	0.8402	1.3675	0.6601		0.003098532	0	242.4796
191	mass fuel	0.00010889		9	0.61917	0.6192	0.9654	1.3675	0.7163		0.003098532	0	226.6388
192	INJ_Start	-3.75	[kg]	10	0.66634	0.6663	1.0976	1.3675	0.7725		0.003098532	0	209.4327
193	INJ_Dur	6	[CAD]	11	0.7097	0.7097	1.2368	1.3675	0.8287		0.003098532	0	191.4873
194	INJ_mass	1.8149E-05	[deg]	12	0.7491	0.7491	1.3827	1.3675	0.8848		0.003098532	0	173.3387
195	LHV_Die	4.25E+07		13	0.7846	0.7846	1.5352	1.3675	0.9410		0.003098532	0	155.4326
196	Energy Released	4627.92543	[j]	14	0.8163	0.8163	1.6943	1.3675	0.9972		0.003098532	0	138.1259
197	Max Energy RL	4628		15	0.8443	0.8443	1.8597	1.3675	1.0534		0.003098532	0	121.6923

Figure 11 - Combustion Tab from the 0D Model
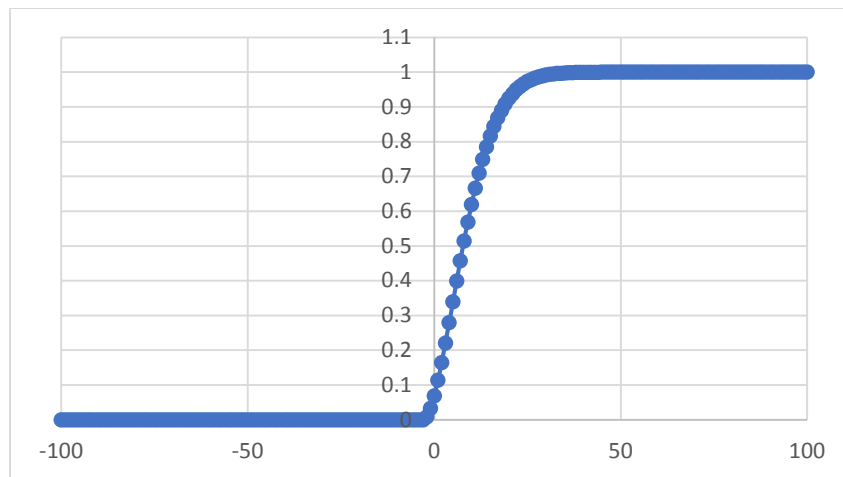
Figure 12 - Resulting x$_{b,i}$ *Graph for Simulation Model*

For the energy lost due to heat transfer, Equation 6, the temperatures were kept consistent with the paper as well. This was done due to the values being consistent with other sources and because the size of the cylinders were similar [14]. For Equation 7, the m_{ht} value was chosen to be .8 as in order to match the given value from Heywood [12]. In Equation 8, the reference temperature, volume and pressure were chosen to be the at the time the valves closed. These values were then 350K, 1.72L and 1.75bar. A screenshot of the tab used for heat transfer calculations with these constants can be seen in Figure 13.

	Bore	0.1 [m]		Crank Angles	A-liner [m^2]	Temperature [K]	Pressure [Pa]	[Bar]	dPdTheta [Pa]	dQHTdTheta [J]	hci [W/(m^2 K)]	wi [m/s]	dQCdTheta [J]	Motoring V1	Motor Pressure [Bar]		Work
Bore	0.1 [m]		-130	0.06864213	348.4498153	175000	1.75	1743.251184	-0.156272014	332.9999719	34.2	0	1706.984663	175000	1.75		0
R	3.50		-129	0.068158876	349.4432794	176743.2512	1.77	1800.640048	-0.155215582	335.1258897	34.2	0	1764.060021	176706.9847	1.77		-2.15243815
mht	0.8		-128	0.067667864	350.4603562	178543.8912	1.79	1859.958273	-0.154134102	337.3148739	34.2	0	1823.052259	178471.0447	1.78		-2.20884172
C1	2.28		-127	0.067169162	351.5014859	180403.8495	1.8	1921.293623	-0.153027084	339.5686504	34.2	0	1884.049102	180294.0969	1.8		-2.26637735
C2	0		-126	0.06666284	352.5671214	182325.1431	1.82	1984.738271	-0.15189402	341.8890129	34.2	0	1947.162705	182178.146	1.82		-2.32507871
C3	3.25E-03		-125	0.066148972	353.6577287	184309.8814	1.84	2050.389053	-0.150734385	344.2778249	34.2	0	2012.429915	184125.2887	1.84		-2.38498045
Vd	0.0017167 [m^3]		-124	0.065627635	354.7737869	186360.2705	1.86	2118.347755	-0.149547636	346.7370235	34.2	0	2080.01256	186137.7187	1.86		-2.44611821
Tr	350 [K]		-123	0.065098912	355.9157888	188478.6182	1.88	2188.721409	-0.14833321	349.268622	34.2	0	2149.997748	188217.7312	1.88		-2.50852868
Vr	0.0017161 [m^3]		-122	0.064562887	357.0842412	190667.3396	1.91	2261.622608	-0.147090526	351.8747133	34.2	0	2222.498188	190367.729	1.9		-2.57224965
Pr	175000 Pref		-121	0.06401965	358.2796654	192928.9622	1.93	2337.169846	-0.145818978	354.5574733	34.2	0	2297.632538	192590.2272	1.93		-2.63732003
N	3600 [rpm]		-120	0.063469295	359.5025971	195266.1321	1.95	2415.487883	-0.144517944	357.319165	34.2	0	2375.525774	194887.8597	1.95		-2.70377993
Sp	15 [m/s]		-119	0.062911919	360.7535875	197681.62	1.98	2496.708128	-0.143186774	360.1621416	34.2	0	2456.309579	197263.3855	1.97		-2.77167066
Aip	0.007854 [m^2]		-118	0.062347624	362.0332029	200178.3281	2	2580.969054	-0.141824797	363.0888512	34.2	0	2540.122767	199719.6951	2		-2.84103485
Aep	0.007854 [m^2]		-117	0.061776517	363.342026	202759.2971	2.03	2668.416639	-0.140431317	366.1018407	34.2	0	2627.111731	202259.8178	2.02		-2.91191646
Tip	550 [K]		-116	0.061198709	364.6806554	205427.7138	2.05	2759.204838	-0.139005612	369.2037605	34.2	0	2717.430929	204886.9295	2.05		-2.98436084
Tep	550 [K]		-115	0.060614313	366.049707	208186.9816	2.08	2853.49609	-0.137546931	372.397369	34.2	0	2811.243394	207604.3605	2.08		-3.0584148
Tl	450 [K]		-114	0.060023451	367.7498136	211040.4147	2.11	2951.461854	-0.136054495	375.685538	34.2	0	2908.721289	210415.6039	2.1		-3.13412667
Rho_Air	1.7421603 kg/m^3		-113	0.059426247	368.8816259	213991.8766	2.14	3053.283192	-0.134527498	379.0712576	34.2	0	3010.046498	213324.3252	2.13		-3.21154635
ma_cylinder	0.0029775 [kg]		-112	0.058822828	370.345813	217045.1597	2.17	3159.151389	-0.132965097	382.557642	34.2	0	3115.411262	216334.3717	2.16		-3.29072541
Theta_Time	4.63E-05 [s]		-111	0.058213328	371.8430628	220204.3111	2.2	3269.268616	-0.13136642	386.1479353	34.2	0	3225.01886	219449.7829	2.19		-3.37171714
Pressure start	1.75 [bar]		-110	0.057597886	373.3740824	223473.5798	2.23	3383.848642	-0.129730559	389.8455178	34.2	0	3339.084335	222674.8018	2.23		-3.45457661
Cell Start	52		-109	0.056976645	374.9395989	226857.4284	2.27	3503.117599	-0.128056568	393.6539125	34.2	0	3457.835283	226013.8861	2.26		-3.53936079

Figure 13 - Heat Transfer Tab for 0D Model

For Equation 15, the x_{no} and x_{bo} values were determined from the simple combustion equation assuming no dissociation and frozen cylinder contents. The constituents in the equation were diesel fuel, nitrogen and oxygen and they combust to form water and carbon dioxide. Because the engines run lean, there was excess nitrogen and oxygen on the results side of the combustion equation. In order to account for this, the gamma tab of the model was constructed so that if the lambda value changed, the values of the pre- and post-combustion mole fractions changed accordingly.

For the volume tab, little was changed. For the volume tab, the new dimensions simply needed to be input. For the inputs in Equation 17, the compression ratio was deemed to be 18 as that is a relatively standard compression ratio for diesel engines and it was successfully used in the Junkers Jumo engine [4,12]. The value of R was kept at 3.5 as that is a standard value for medium to large sized engines [12]. The volume tab can be seen in Figure 14. The graph of the volumes can be seen in Figure 15.

|	[L]	[m^3]	Intake - Exhaust - Cr	Crank Angle	Exhaust - C		S-Length Intake	S-Length Exhaust	IntakeHalf-Volume	Exhaust Half-Volume	Volume	Volume [L]	dVdTheta
			-180	-166.5	-3.141593	-2.90597	0.15625	0.15748976	0.001032239	0.001022502	0.00205474	2.054740712	0
			-179	-165.5	-3.124139	-2.88852	0.1562568	0.157680321	0.001032185	0.001021005	0.00205319	2.053190643	-1.65702E-06
rc	18		-178	-164.5	-3.106686	-2.87107	0.156277198	0.157884519	0.001032025	0.001019401	0.00205143	2.051426668	-1.87095E-06
Vd	1.7167	0.0017167	-177	-163.5	-3.089233	-2.85361	0.156311197	0.158102356	0.001031758	0.001017691	0.00204945	2.04944875	-2.08491E-06
Vc	0.100982353	0.000100982	-176	-162.5	-3.071779	-2.83616	0.156358796	0.158333838	0.001031384	0.001015872	0.00204726	2.047256849	-2.29891E-06
Vc for half	0.050491176	5.04912E-05	-175	-161.5	-3.054326	-2.81871	0.156419998	0.158578968	0.001030904	0.001013947	0.00204485	2.044850924	-2.51296E-06
Other Variables			-174	-160.5	-3.036873	-2.80125	0.156494804	0.15883775	0.001030316	0.001011915	0.00204223	2.042230931	-2.72705E-06
Stroke	0.125 [m]		-173	-159.5	-3.01942	-2.7838	0.156583217	0.159110187	0.001029622	0.001009775	0.00203940	2.039396826	-2.94118E-06
R	3.50		-172	-158.5	-3.001966	-2.76635	0.156685238	0.159396282	0.001028821	0.001007528	0.00203635	2.036348563	-3.15536E-06
bore	0.1		-171	-157.5	-2.984513	-2.74889	0.156800872	0.159696039	0.001027912	0.001005174	0.00203309	2.033086099	-3.36959E-06
a	0.0625		-170	-156.5	-2.96706	-2.73144	0.15693012	0.160009458	0.001026897	0.001002712	0.00202961	2.029609393	-3.58385E-06
l	0.21875		-169	-155.5	-2.949606	-2.71399	0.157072987	0.160336543	0.001025775	0.001000143	0.00202592	2.025918404	-3.79815E-06
Step	1		-168	-154.5	-2.932153	-2.69653	0.157229476	0.160677293	0.001024546	0.000997467	0.00202201	2.022013097	-4.01248E-06
Phase Shift	13.5		-167	-153.5	-2.9147	-2.67908	0.157399591	0.161031709	0.00102321	0.000994683	0.00201789	2.01789344	-4.22684E-06
Start Cell	52		-166	-152.5	-2.897247	-2.66163	0.157583336	0.16139979	0.001021767	0.000991793	0.00201356	2.013559408	-4.44123E-06
			-165	-151.5	-2.879793	-2.64417	0.157780715	0.161781534	0.001020217	0.000988794	0.00200901	2.009010984	-4.65563E-06
			-164	-150.5	-2.86234	-2.62672	0.157991732	0.162176939	0.001018559	0.000985689	0.00200425	2.004248156	-4.87003E-06
			-163	-149.5	-2.844887	-2.60927	0.158216392	0.162586001	0.001016795	0.000982476	0.00199927	1.999270926	-5.08443E-06
			-162	-148.5	-2.827433	-2.59181	0.158454697	0.163008713	0.001014923	0.000979156	0.00199408	1.994079304	-5.29881E-06
			-161	-147.5	-2.80998	-2.57436	0.158706652	0.16344507	0.001012944	0.000975729	0.00198867	1.988673314	-5.51316E-06
			-160	-146.5	-2.792527	-2.55691	0.158972261	0.163895062	0.001010858	0.000972195	0.00198305	1.983052992	-5.72746E-06
			-159	-145.5	-2.775074	-2.53945	0.159251527	0.164358681	0.001008665	0.000968553	0.00197722	1.977218394	-5.9417E-06

Figure 14 - Volume Tab for 0D Model
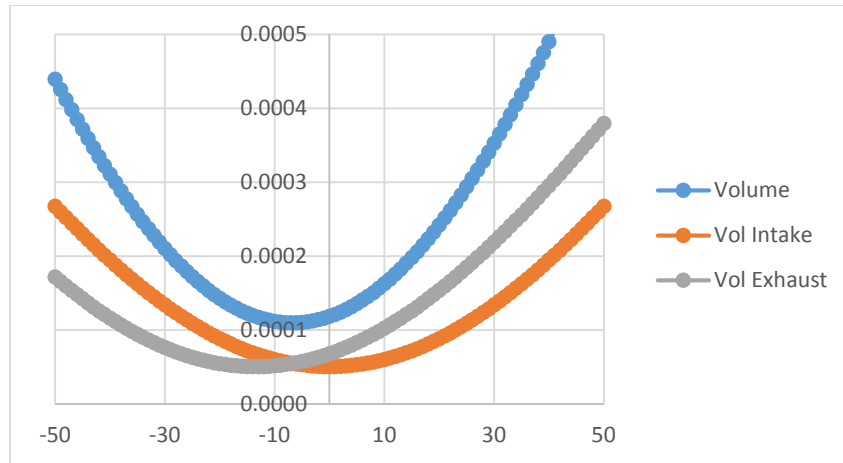
Figure 15 *- Volumes for 0D Model*

For the coefficients tab, the chart of the specific heat coefficients that was provided in the literature is included on the left-hand side of the spreadsheet [12]. Equation 11 was the only equation on the tab which was used in Figure 16.

		N2	O2	CO2	H2O	Ar
T<1000K	a1_10	2.21E+04	-3.43E+04	4.94E+04	-3.95E+04	0.00E+00
	a2_10	-3.82E+02	4.85E+02	-6.26E+02	5.76E+02	0.00E+00
	a3_10	6.08273836	1.12E+00	5.30E+00	9.32E-01	2.50E+00
	a4_10	-8.53E-03	4.29E-03	2.50E-03	7.22E-03	0.00E+00
	a5_10	1.38E-05	-6.84E-07	-2.13E-07	-7.34E-06	0.00E+00
	a6_10	-9.63E-09	-2.02E-09	-7.69E-10	4.96E-09	0.00E+00
	a7_10	2.52E-12	1.04E-12	2.85E-13	-1.34E-12	0.00E+00
T> 1000K	a1_20	5.88E+05	-1.04E+06	1.18E+05	1.03E+06	2.01E+01
	a2_20	-2.24E+03	2.34E+03	-1.79E+03	-2.41E+03	-5.99E-02
	a3_20	6.06694922	1.82E+00	8.29E+00	4.65E+00	2.50E+00
	a4_20	-6.14E-04	1.27E-03	-9.22E-05	2.29E-03	-3.99E-08
	a5_20	1.49E-07	-2.19E-07	4.86E-09	-6.84E-07	1.21E-11
	a6_20	-1.92E-11	2.05E-11	-1.89E-12	9.43E-11	-1.82E-15
	a7_20	1.06E-15	-8.19E-16	6.33E-16	-4.82E-15	1.08E-19
R_N2	296.8					
R_CO2	188.9					
R_O2	259.8					
R_H2O	461.5					
R_Ar	208.1					

Crank Angle	cpi_N2 [W/(m^2 K)]	cpi_O2 [W/(m^2 K)]	cpi_CO2 [W/(m^2 K)]	cpi_H2O [W/(m^2 K)]	cpi_Ar [W/(m^2 K)]
-130.00	1041.010	927.697	893.397	1879.968	520.250
-129.00	1041.051	927.926	894.324	1880.341	520.250
-128.00	1041.094	928.161	895.271	1880.725	520.250
-127.00	1041.139	928.403	896.238	1881.120	520.250
-126.00	1041.185	928.653	897.225	1881.527	520.250
-125.00	1041.234	928.909	898.234	1881.946	520.250
-124.00	1041.284	929.174	899.263	1882.377	520.250
-123.00	1041.336	929.445	900.314	1882.821	520.250
-122.00	1041.391	929.725	901.386	1883.279	520.250
-121.00	1041.447	930.013	902.480	1883.750	520.250
-120.00	1041.506	930.309	903.596	1884.235	520.250
-119.00	1041.568	930.614	904.734	1884.734	520.250
-118.00	1041.632	930.928	905.895	1885.248	520.250
-117.00	1041.698	931.251	907.080	1885.778	520.250
-116.00	1041.768	931.583	908.287	1886.323	520.250
-115.00	1041.840	931.924	909.519	1886.884	520.250
-114.00	1041.915	932.276	910.774	1887.461	520.250
-113.00	1041.994	932.637	912.054	1888.056	520.250
-112.00	1042.076	933.009	913.358	1888.669	520.250
-111.00	1042.161	933.392	914.688	1889.299	520.250
-110.00	1042.250	933.786	916.042	1889.948	520.250

Figure 16 *- Specific Heats Tab*

By taking the lambda value of 1.9 from the 0D model and using Equation 22, the mass flow rate of air could be determined, and this resulted in a mass flow rate of 143lb/min. Because turbochargers work within a specified range of pressure ratios relative to mass flow rate, one needs to ensure that during the entire operating cycle it is operating within its map. The pressure ratio is defined as the ratio of the air pressure entering the cylinder to the air pressure entering the turbocharger [12, 13]. Since turbochargers are engineered devices of their own merit, one was simply picked off the shelf to be used in conjunction with this engine. The turbocharger chosen was the Garrett GTX5533R II with a 98mm inducer, Figure 17.
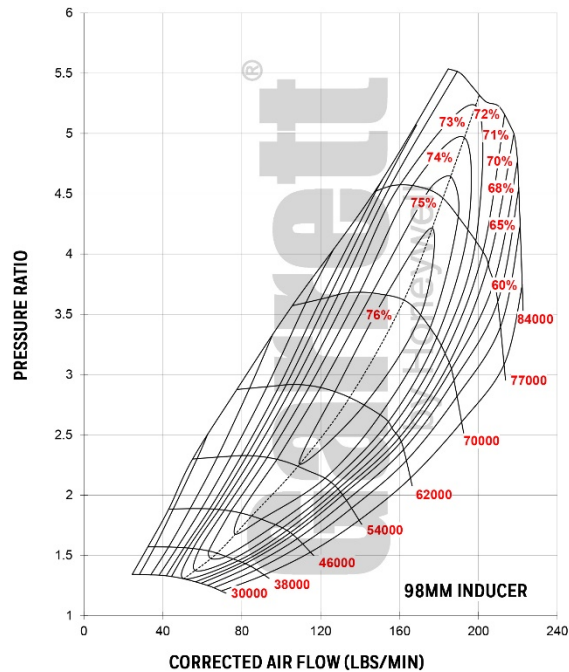
Figure 17- Garrett GTX5533R II (adapted from [15])

Along with the changes that were calculated due to the ports, the starting pressure was adjusted in order to account for the attachment of a turbocharger. In order to use the Garrett turbocharger, the minimum pressure ratio has to be 1.75 in order to operate at the desired mass flow rate. If the pressure ratio drops below this value, the turbocharger falls out of its map and chokes [13]. At low pressure ratios like takeoff, the turbo will work in its lowest efficiency but as the engine would climb in altitude, the pressure ratio will increase due to the reduction in atmospheric pressure and the efficiency will climb into its maximum range. This results in the initial pressure at sea level needing to be at least 1.75bar [15].

Once this was accounted for, the 0D model was run in order to determine the power output of the engine. Assuming a pressure ratio of 1.75 and an in-cylinder pressure of 1.75bar, the engine will generate 204.01hp per cylinder and 1224.08hp for all six cylinders. The maximum pressure rise rate is 3.94bar/CAD and the mean effective pressure was 214.22psi. These results can be seen in Figure 18. The nominal value according the Heywood text is that a diesel engine should have a mean effective pressure of 140psi at maximum rated power. However, mean effective pressures over 200psi are not uncommon for turbocharged, aftercooled diesel engines [12]. While this value is higher than what was expected, it is not abnormal compared to other boosted engines.

Additionally, the mean effective pressure returns to expected values when calculated with the assumed level flying characteristics. The FAAT specified that the aircraft should reduce its engine speed to 1800rpm during cruising. Because of this the engine will generate a different mean effective pressure since it is no longer operating at maximum power and maximum engine speed. Therefore, it is expected that the mean effective pressure will drop to 208.83psi during level flight at altitude. This value fits more closely to what is presented in the textbook by Heywood [12].

Results from 0D Model for FAAT Engine	
Fuel Mass (mg/cycle/cyl)	108.90
$\Delta\theta_{10-90}(\deg)$	17.80
Max Pressure [bar]	98.48
Max Temperature [K]	1960.32
Trapped Lambda	1.90
Power [hp]	1224.08
MPRR	3.94
MEP	214.22
Cylinder Pressure [bar]	1.75

Figure 18 - Results for the Sized Engine

After the turbocharger was sized, a weight estimate could be made. The Junkers Jumo 207B had a density of 1.88lb/in3 and a total weight of 1907lb [OPE]. According to Taylor's textbook, the average two-stroke diesel engine has a density of 2.75lb/in3. Using these two densities as aircraft optimized and unoptimized values, the engine sized in this thesis should fall within the weight range of 1413-2064lb. What this means is that even if the engine is unoptimized it would still weigh nearly as little as the Junkers engine while producing potentially 224 additional horsepower. If it is assumed that the engine could be optimized to match the Junkers density it would mean that this engine would weigh nearly 500lb less than the Junkers.

Along with the weight estimation, an indicated fuel consumption could be calculated using Equation 25. This value is especially important for aircraft engines as it helps show how well the engine is using its fuel. It was determined that the indicated specific fuel consumption is 155g/kWh. This value is an indicated value because it does not factor in losses incurred due to devices attached to the engine itself like the propeller, friction, or other engine add-ons. This means that the actual or brake specific fuel

consumption will be higher than the indicated value. However, because the Junkers brake specific fuel consumption was 227 g/kWh at its most efficient operating parameters, it is reasonable to assume that the engine sized in this thesis will have a comparable or better brake specific fuel consumption than that of the Junkers [4].

Because of the values calculated, it can reasonably be assumed that the engine sized in this thesis will be able to outperform the Junkers engine and satisfy the utility aircraft requirements set by the FAAT. Along with the power output, the engine has a total volume of 12.3L which is four liters or 25% smaller less than the size of the Junkers engine. This means that this engine should also be significantly lighter than its Junkers predecessor. Therefore, the engine outlined in this thesis when built should meet the requirements of the FAAT.

IV. Design Model

Once the results of the simulation model were calculated, the design model could be constructed. The purpose of the design model was to outline the functionality of the engine itself. Because of this, it was limited to being a single cylinder instead of the complete six. By limiting the model to a single cylinder, one can more easily see the inner workings of the engine and how it would function. A complete picture of the model can be seen in Figure 19. The model was made up of several components: the Garrett GTX5533R GEN II turbocharger, the propeller and gear train assembly, the engine block, the piston-crankshaft assembly and the cylinder sleeve.
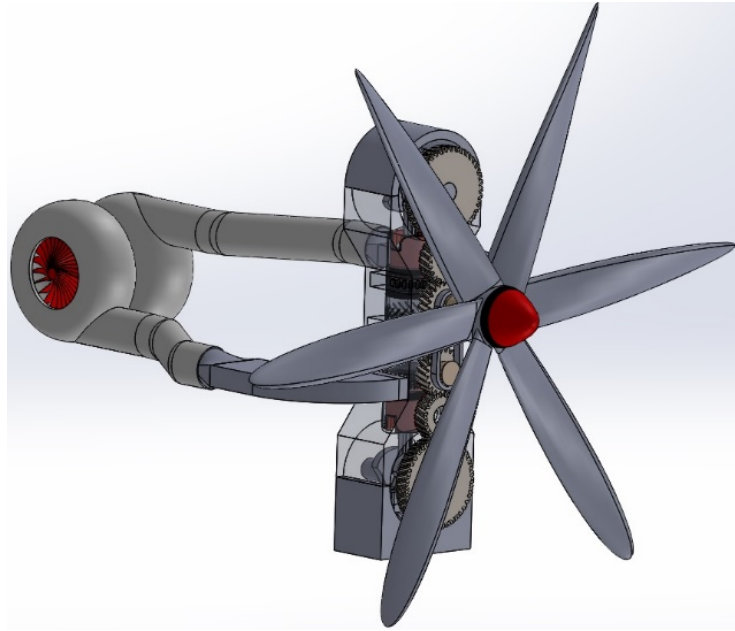
Figure 19 - Full constructed single cylinder design model

Because the turbocharger is its own engineered component, it was not designed as a part of this thesis. In order to help facilitate scavenging and maintain power output at altitude, a turbocharger is recommended. In the field of aviation, there are two types. The first is the turbonormalized turbocharger which simply boosts the engine back to its sea level power as the aircraft climbs in altitude. The second is a turbobooster which increases the intake pressure so that the power output is increased at all altitudes [16]. Because turbonormalizers are constructed for specific aircraft, specifications for these devices were unable to be found. Because of this, a turbobooster was selected from the known manufacturer Garrett as it advertised the compressor map and other specifications needed for operation with each model. Along with the mass flow rate that was calculated in section 3 of this paper, the recommended horsepower and displacement of each turbocharger was looked at to verify the selection. Through this process, the Garrett GTX5533R GEN II was chosen for the purposes of this thesis. The compressor map of the turbocharger can be seen in Figure 17 from section 3 and the dimension drawing can be seen in Figure 20. For the design model, the turbocharger was reconstructed to show its overall dimensions relative to those of the cylinder. Because of this, the outer dimension from the drawing were focused on.
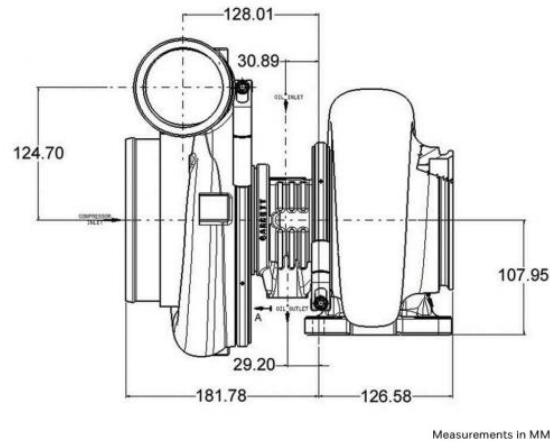
Figure 20 - *Garrett GTX5533R GEN II Turbocharger (adapted from [15])*

The propeller used in the design model was constructed to simply show the connection between the crankshafts and the propeller shaft. The model of the Propeller can be seen in Figure 21. Because the engine design has two crankshafts, the propeller could not be hooked up to either directly without losing the power from the other crankshaft. With this in mind, the propeller needed to be situated towards the center of the engine. Slightly above the center was chosen for two reasons. The first was to replicate the structure of Junkers engine. The Junkers had the propeller situated closer to top crankshaft, and the bottom crankshaft would run the blower and other engine add-ons which meant that the power distribution from the crankshafts was about equal. Additionally, it was organized in this fashion to demonstrate the idea from the FAAT that instead of using a full gear train, a belt could be used in order to further reduce weight. The gear train was constructed with two purposes. The first was to demonstrate how and where the propeller would be connected relative to the crankshafts and the second was to demonstrate the reduction that the FAAT suggested. Because the engine speed of 3600rpm is too high for a propeller to operate at, the FAAT suggested a gear reduction of 2:1 which was similar to reductions used in the Junkers family of engines [4]. Therefore, to reflect this reduction, the pinion is half the size of the gear that connects to the belt and propeller. Additionally, helical gears were chosen for their better power transfer. The gear and belt assembly can be seen in Figure 22.
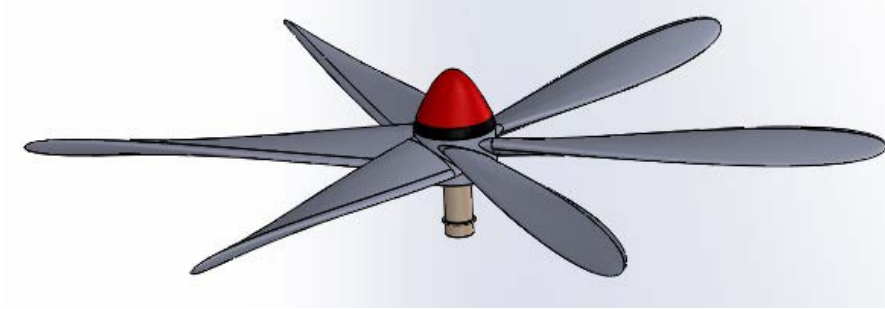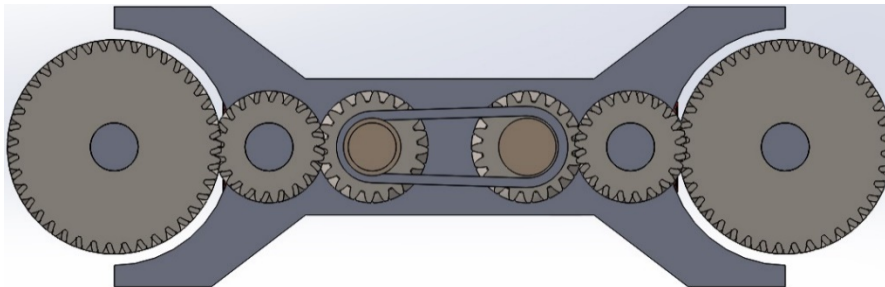
Figure 21 *- Propeller Model*

Figure 22 *- Gear and Belt Train with a 2:1 reduction*

The engine block was created to show the total height of the engine along with dimensions that would be necessary for each cylinder along with locations for the cuts for the ports and fuel injectors. The locations for the cuts for the ports and fuel injectors were chosen so that they line up with the raised rib on the cylinder sleeve on which the ports are cut. The port cuts were dimensioned as to allow a gap of 12mm around the entire cylinder sleeve. This allows the air to enter the cylinder from all sides instead of only at the opening which should assist with better scavenging. The extrusions on the right side of the cylinder where the locations where the gears were mounted. The outline of the center portion of the engine block with the locations of its features can be seen in Figure 23. The top and bottom were simply constructed as to not create interference with the rotating crankshaft. An image of the fully constructed cylinder block can be seen in Figure 24.
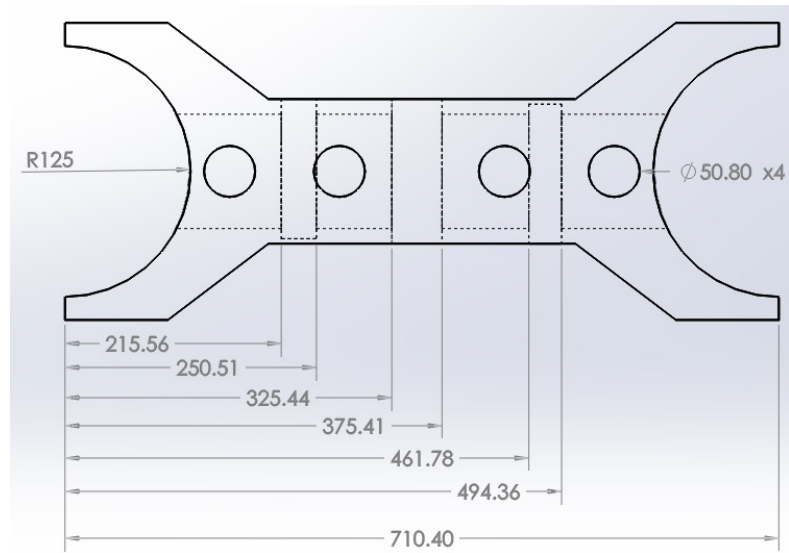
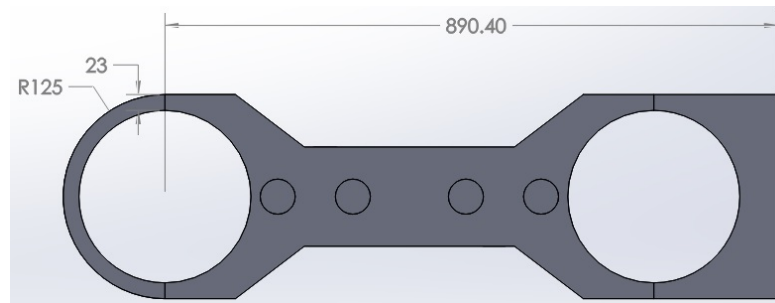***Figure 23*** *- Outline of the center portion of the Engine Block (dimensions are in mm)*

Figure 24 *- Side View of Full Engine Block*

The piston-crankshaft assembly was made up of three parts. The two crankshafts, the two pistons and the two connecting rods. The crankshafts were sized using the stroke length. Because the crank throw is one-half the stroke length, it was 62.5mm. The design of the crankshaft was outlined so that it reflected a standard crankshaft with a counterweight. Using the SolidWorks center of mass tool, the size of the counterweight was adjusted so that the center of mass of the crankshaft was at the center of the rod about which the crankshaft rotates. This can be seen in Figure 25. The connecting rods were constrained by the ratio of the connecting rod to the crank throw which was previously defined to be 3.5. Therefore, the length of the connecting rod was 218.76mm long. The connecting rod was built in two pieces in order to represent how it would be assembled in the engine. The smaller hole is in one piece as the piston pin, which connects the piston to the connecting rod, simply slides though it. The larger hole is cut into two pieces as it is assembled by bolting the two pieces together around the

crankshaft. The connecting rod can be seen in Figure 26. The piston was constructed to represent a standard piston geometry. Its diameter was 99mm so that there was a 1mm gap between the piston and cylinder walls. This gap would be filled with the piston rings whose notches were cut closer to the top of the piston. The purpose of the piston rings are to minimize the contact that exists between the moving piston with the cylinder liner. This minimizes friction and wear. Additionally, the piston rings have the function of preventing combustion gases from escaping around the piston thereby maximizing the pressure that is exerted against the piston. The piston can be seen in Figure 27. It was painted red in order assist with its visibility within the entire assembly. The full assembly can be seen in Figure 28. The cylinder sleeve was included to allow the offset to be visible. The crankshafts in this model are offset by 13.5 degrees which allow the exhaust to open before the intake. This can be seen because the piston on the right has nearly reached the fuel injector while the left piston has not passed the ribbing.
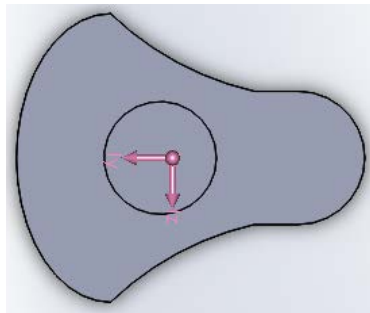

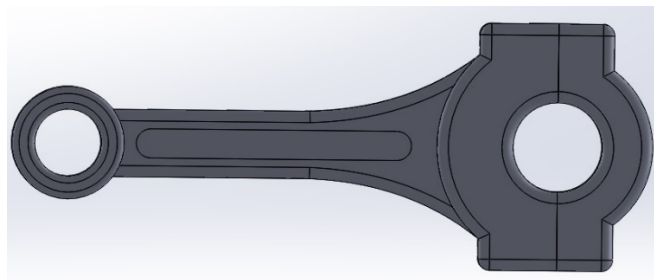*Figure 25 - Crankshaft with the location of the center of mass*

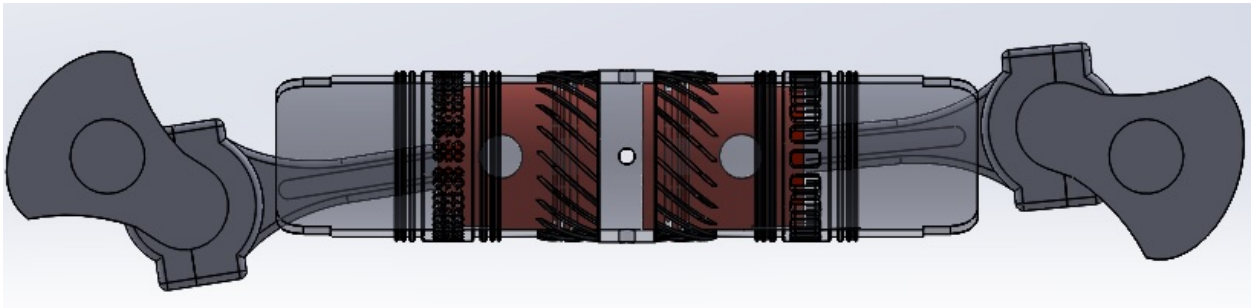*Figure 26 - Connecting Rod*

Figure 27 – Piston

Figure 28 - Full Piston Crankshaft Assembly

The cylinder sleeve is the final component of the assembly and can be seen in Figure 29. It is made up of four features. The first are the notches cut on the ends of the sleeve. These serve the purpose of allowing the connecting rod to rotate about the crankshaft without coming into contact with the cylinder sleeve itself. The next component were the intake and exhaust ports. Although the total area of the intake and exhaust ports were calculated in section three, the length of the ports were determined by the 0D model and at which crank angles the trapped volume was 1.72L. Because of this, the ports needed to open and close at ±130 degrees. This resulted in the exhaust port beginning at 112.41mm away from the center of the sleeve. The length of the port was 19mm and it had a width of 10mm. In order to easily distinguish the intake and exhaust ports from each other, the exhaust ports were made rectangular while the intake ports were made to be a series of small holes. This was also consistent with the Junkers engine. The intake ports with the limit of beginning and ending at ±130 CAD began at 112.69mm from the center of the sleeve and end at 131.49mm from the center of the sleeve. The slight difference in distances is a result of the difference port geometries. The third component of the cylinder sleeve was the fuel injectors. It is assumed that the

fuel injector will be inserted into the sleeve via a tapped hole. For this purpose, a standard M12x1.25 hole was tapped into the model to demonstrate where these injectors would be placed. The final component was the series of ribs around the cylinder. Because of the nature of combustion, the lower the temperatures can be kept during and after combustion the greater the work that can be extracted as lower temperatures allow the gamma value to remain higher. In order to help reduce the internal temperatures, ribs were created around the sleeve in order to help facilitate the heat transfer out of the cylinder.
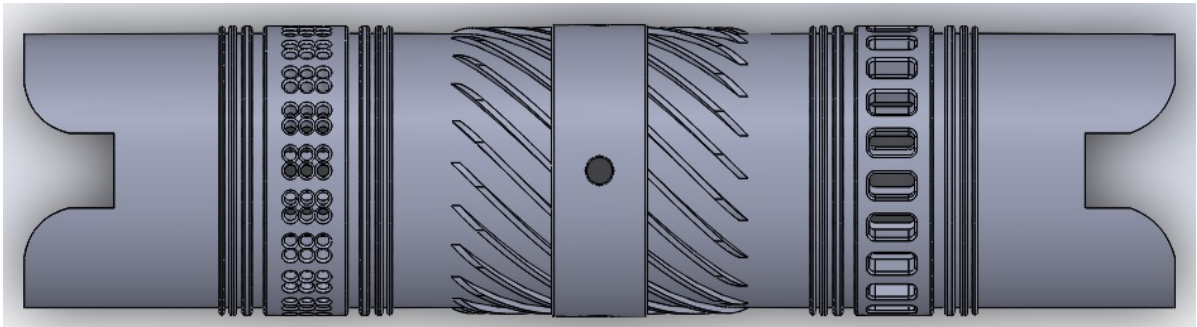

Figure 29 - *Top View of the Cylinder Sleeve*

V. Conclusions and Recommendations

The 0D model demonstrates that an opposed-piston, two-stroke diesel engine could be constructed to meet the requirements of the Foundation for Applied Aviation Technology and that further research should be conducted in order to more fully develop a model for this engine. Opposed-piston, opposed-two-stroke diesel engines provide a number of benefits that allow the engine to be lighter, more fuel efficient, and less complicated. The Junkers Jumo family of engines set a number of records, and for a significant period of time, was one of the most advanced engines of its time [4]. It was very lightweight for an opposed-piston, two-stroke engine in the sense that it is almost a pound lighter per cubic inch than the 2.75lb/in^3 estimate provided by Taylor [13]. It also obtained 1000hp while at the same time having a lean brake specific fuel consumption of 227g/kWh [4]. Along with the benefits that are illustrated by the Junkers' success, literature demonstrates that the opposed-piston, two-stroke architecture exhibits an inherent 9% fuel economy benefit over the standard 4S design and the opposed-piston,

four-stroke design. This results from the inherent lean combustion of the two-stroke, diesel design [7].

The initial dimensions for this engine were gathered using standard mean effective pressure values and guidelines for the mean piston speed. By reconstructing the 0D model that was in the literature, the dimensions for the engine sought by the FAAT could be verified by relating the change in pressure throughout the cycle with the energy released by combustion and the energy lost due to heat transfer and the cylinder contents changing [7]. After validating this model against an engine from the literature, the model could be used to show whether or not Equations 1 and 2 accurately predicted the dimensions and output of the engine desired by the FAAT. Further calculations, determined the dimensions of the intake and exhaust ports along with the mass flow rate required for the turbocharger. Once these values were determined the 0D model could then be used to verify power output of the modeled engine. While the 0D model does not factor in friction losses, it still demonstrates that a power output significantly higher than the requirements of the foundation is possible. The model showed an output of 1224hp and a specific fuel consumption of 155g/kWh. Both of these values are substantially better than the Junkers 207B engine. Additionally, due to the size reduction, a potential weight reduction of up to 500lb is possible assuming that the engine can be optimized for aviation. Once the model was run and results calculated, a design model was created in order to show how each of the components work together.

Moving forward, a couple of things are recommended. The first would be to re-validate the excel sheet in order to see if it is possible to fix the deviation of pressure values around the combustion zone compared to the literature simulation. Additionally, the 0D model should be expanded to include friction. This will allow a more accurate indicated power to be determined. A finite element analysis should be conducted in order to see how small the full engine can be made as this would result in the maximum weight savings. Lastly, it is recommended that the use of the turbocharger and port flow be researched and a model generated to determine that the air is flowing properly into and out of the cylinder. A potential solution that should be researched is the combination of a turbocharger with a scavenging pump in order to facilitate air flow through the cylinder. It is possible that the turbocharger may by itself not be sufficient. If these

recommendations are followed it is quite possible that the Foundation for Applied Aviation Technology will be able to construct an engine that meets their needs.

VI. Bibliography

[1]   U.S. Government Publishing Office, "Electronic Code of Federal Regulations: Title 14: Aeronautics and Space," 31 March 2017. [Online]. Available: https://www.ecfr.gov/cgi-bin/text-idx?SID=a38b8152e37301d6a2ec0a9d2c42e272&mc=true&node=se14.1.23_13&rgn=div8. [Accessed 31 January 2017].

[2]   B. Cox, "Turbines vs. Pistons," Plane and Pilot, 19 June 2012. [Online]. Available: http://www.planeandpilotmag.com/article/turbines-vs-pistons/#.WOPKkPkrJPZ. [Accessed 1 April 2016].

[3]   "Cessna," Cessna Aircraft Company, 2015. [Online]. Available: http://cessna.txtav.com/. [Accessed 26 March 2016].

[4]   J.-P. Pirault and F. Martin, Opposed Piston Engines: Evolution, Use, and Future Applications, Warrendale, PA: SAE International, 2010.

[5]   J. Parker, S. Bell and D. Davis, "An Opposed-Piston Disel Engine," Journal of Engineering for Gas Turbines and Power, pp. 734-741, 1993.

[6]   J.-P. Pirault and M. Flint, "Opposed-Piston Engine Renaissance: Power for the Future," Achates Power, Inc, San Diego, 2010.

[7]   R. E. Herold, M. H. Wahl, G. Regner, J. U. Lemke and D. E. Foster, "Thermodynamic Benefits of Opposed-Piston Two-Stroke Engines," SAE International, 2011.

[8]   M. Franke, H. Huang, J. P. Liu and A. Geistert, "opposed Piston Opposed Cylinder (opoc) 450 hp Engine: Performance Development by CAE Simulations and Testing," S.A.E. Transactions, pp. 196-203, 2006.

[9]   A. K. Marsh, "Little Diesel, Big Fuel Savings," 2015 February 2015. [Online]. Available: https://www.aopa.org/news-and-media/all-news/2015/february/pilot/f_diesel. [Accessed 3 April 2017].

[10] P. Garrison, "How do Thielert Diesels do It?," 9 October 2004. [Online]. Available: http://www.flyingmag.com/how-do-thielert-diesels-do-it. [Accessed 3 April 2017].

[11] F. Ma, C. Zhao, F. Zhang, Z. Zhao and S. Zhang, "Effects of Scavenging System Configuration on In-Cylinder Air Flow Organization of an Opposed-Piston Two-Stroke Engine," energies, vol. 8, pp. 5866-5884, 2015.

[12] J. B. Heywood, Internal Combustion Engine Fundamentals, Singapore: McGraw-Hill Book Co, 1988.

[13] C. F. Taylor, "The Internal Combustion Engine in Theory and Practice," The Technology Press of The Massachusetts Institute of Technology, New York, 1960.

[14] Ricardo Wave, 4.1.2 Diesel Engine Model, Van Buren Twp.: Ricardo Software, 2016.

[15] Honeywell Garrett Performance Products, "GTX5533R GEN II," Honeywell International Inc, 2017. [Online]. Available: https://www.turbobygarrett.com/turbobygarrett/turbochargers/gtx5533r-gen-ii. [Accessed 1 February 2017].

[16] Shoreline Aviation, "Aircraft Engine Turbochargers Explained," Shoreline Aviation Worldwide Charter & FBO Services, 19 March 2012. [Online]. Available: http://www.shorelineaviation.net/news---events/bid/57041/Aircraft-Engine-Turbochargers-Explained. [Accessed 1 February 2017].

[17] L. V. Armstrong and J. B. Hartman, The Diesel Engine: Its theory, Basic Design, and Economics, New York: The Macmillan Company, 1959.

[18] H. B. John and S. Eran, The Two-Stroke Cycle Engine: Its development, Operation, and design, Philidelphia: Taylor & Francis, 1999.

[19] F. Ma, F. Zhao, Z. Zhenfeng, Z. Zhang, Z. Xie and H. Wang, "An Experimental Investigation on the Combustion and Heat Release Characteristics of an Opposed-Pisotn Folded-Cranktrain Diesel Engine," energies, vol. 8, pp. 6365-6381, 2015.